Mechanical Properties of a Ni-Co-Cr-Mo Alloy

Ke Han, Y. Xin, V. J. Toplosky, R. M. Niu, and J. Lu

Abstract—**Because effective reinforcement materials must have both high capacity for load bearing and high resistance to deformation under external force, they require both high mechanical tensile strength and a high elasticity modulus. Both strength and modulus are usually amplified at cryogenic temperatures, so properties at both cryogenic and room temperatures must be characterized before the materials can be used for applications. In this study, we investigated a nickel-based alloy whose Young's modulus is higher than that of the stainless steels that have commonly been relied on as reinforcement materials in cryogenic environments. Our test alloy was subjected to a type of thermo-mechanical processing that strengthens the alloy through very fine planar defects. We first deformed the alloy to various magnitudes at room temperature, and we then measured its properties at both cryogenic and room temperatures. Finally, we assessed the properties (at both temperatures) of the materials that were deformed to different deformation strains at room temperature. We found that our test alloy had anisotropy in both elastic modulus and mechanical strength and had more resistance to plastic deformation at cryogenic temperatures than at room temperatures. We then investigated physical property changes in various magnetic fields and at various cryogenic temperatures. This paper summarizes 1) the changes that occurred in the microstructure of our alloy and 2) the properties desirable for effective reinforcement materials.**

Index Terms—**Mechanical strength, reinforcement, Young's modulus.**

I. Introduction

MP35N^{TM} -35wt%Co-35wt%Ni-20wt%Cr-10wt%Mo is a high-strength, high-modulus, and high-corrosion-resistant material with various applications [1], [2], [3], [4]. MP35N is considered a biomaterial and can be used in applications such as fasteners for the repair of bone fractures [5], [6]. In the 2000s, researchers began using MP35N as reinforcement material for pulsed magnets [7], [8]. MP35N has recently been suggested as an alternative to other Ni-based alloys, such as Hastelloy alloys, for manufacturing superconductors and superconducting magnets [9], [33]. Hastelloy C-276, for example, is composed of nickel, chromium, molybdenum, and tungsten. Its Young's moduli are reported to be 195 GPa at room temperature and up to 212 GPa at cryogenic temperatures [27]. Researchers have also explored the use of Haynes alloys in superconductor magnets [10], [11], [12], [13], [14]. Although these alloys have higher moduli than stainless steels, their strength and moduli are lower than those of MP35N. Due to the unique properties of MP35N, researchers have focused on both characterizing and improving its properties [15], [16], [17].

Received 18 September 2024; revised 5 December 2024; accepted 15 January 2025. Date of publication 11 March 2025; date of current version 2 April 2025. This work was supported by the National Science Foundation under Cooperative Agreement DMR-1644779 and Cooperative Agreement DMR-2128556 through the National High Magnetic Field Laboratory (NHMFL) and in part by the State of Florida. *(Corresponding author: Ke Han.)*

The authors are with National High Magnetic Field Laboratory, Tallahassee, FL 32301 USA (e-mail: han@magnet.fsu.edu).

Color versions of one or more figures in this article are available at https://doi.org/10.1109/TASC.2025.3541999.

Digital Object Identifier 10.1109/TASC.2025.3541999

MP35N can be used in an annealed condition [18]. In this condition, the alloy takes the form of a solid solution with a face-centred-cubic (fcc) structure. MP35N is hardened by cold deformation. In this condition, MP35N was described as a multiphase cobalt-nickel alloy [19], [20], [21], [22], [23], [24]. The second major phase manifested by this alloy has been found to display a hexagonal-close-packed (hcp) structure. The lack of evidence for an hcp phase in a cold-deformed quaternary alloy like MP35N, however, suggests that its strengthening mechanisms and phase transformations require further investigation [16], [25], [26], [27]. In binary cobalt-nickel alloys, for example, it has not been possible to use X-ray diffraction techniques to detect a stress-induced hcp phase [28].

Several researchers have attributed the strengthening of MP35N to the production of deformation twins in the fcc matrix [29], [30], [31]. Some researchers have reported the absence of hcp, and they have attributed the alloy's strength to dispersed, nanosized γ' phase particles [28]. Recent studies have revealed that most of the planar defects or stacking faults that strengthen the fcc matrix of MP35N are produced by deformation [32].

Aging strengthens cold-deformed MP35N significantly [21], [22]. There are optimized aging times and temperatures for the maximization of mechanical strength [7], [30]. Various researchers have found that, to produce age-hardening, it is necessary to deform MP35N beforehand; otherwise, aging alone will not strengthen this material [21], [22]. In contrast, most other age-hardened nickel-based materials can be hardened either with or without prior deformation [33], [34]. To resolve this contradiction, it will be necessary to explore the relative effects on hardening brought about in MP35N by various combinations of deformation and aging. To understand the hardening mechanisms involved, it will be necessary to identify any phase transformation resulting from any possible combination of deformation and aging. This paper will review existing research concerning the deformation mechanisms and the resulting microstructure changes that occur in MP35N.

Even though MP35N is generally known to have good cryogenic mechanical properties, very little detailed research has been undertaken so far on its deformation mechanism at cryogenic temperatures [9], [29], [35], [36], [37], [38]. This paper is particularly focused, not only on cryogenic properties, but also on the microstructure changes induced by cryogenic deformation of MP35N. All tests, therefore, were done at both room temperature and at 77K.

II. Experimental Methods

A. Materials

MP35N plates and sheets, which were rolled to reduction-in-thickness of 45%, 55%, 65%, and 70%, were supplied for this study by H.C. Starck of Cleveland, OH. The fact that the rolling process itself introduced almost no change in width indicated that rolling had occurred under biaxial stress. The rolled materials were subjected to aging heat treatment at 820 K–850 K in a furnace retort. Samples were heat-treated under flowing argon, some for 4 hours and some for 8 hours.

Samples were machined with the tensile axis either parallel to the longitudinal direction of cold rolling, or parallel to the transverse direction, or perpendicular to the rolling plane.

B. Tensile Tests

Tensile tests were conducted according to the guidelines given in ASTM E 8M. All tests were done either with a 100 kN capacity servo-hydraulic MTS test machine equipped with a cryostat or 250 N Tytron. The tensile-test specimen was attached to the test machine using bolt-together grips. Strain was recorded by a clip-on extensometer with a gauge-length of 25 mm in MTS test machine or by a digital imaging correlation system. Force was recorded by either a 100 kN load cell or 250 N load cell. Tests were conducted at an actuator stroke rate of 0.5 mm/min. Whenever an accurate measurement of the modulus of elasticity was needed, we instructed the program to perform the unload/reload cycle after the observed onset of plastic strain (typically 1.5 to 2.0% strain) and then to load the specimen further until failure. Samples were tested at either room temperature (295 K), or liquid nitrogen temperature (77 K), or liquid helium temperature (4 K).

C. Microstructure Examinations

We prepared transmission electron microscopy specimens ground to a thickness of about 50 μm. From each, a 3 mm diameter disk was punched out and subsequently ion- or jet-polished. In order to study strengthening mechanisms, the microstructure and composition of the samples were observed using a JEOL JEM-ARM200cF Transmission Electron Microscope (TEM), equipped with an Oxford Aztec Energy-dispersive spectroscopy (EDS) detector [39], [40].

III. Results

A. Mechanical Properties

Materials showed anisotropy in mechanical strength. In plate samples deformed to 45%, for example, Ultimate Tensile Strength (UTS) and Yield Strength (YS) had the highest values in Transverse Direction (TD) and the lowest values in Normal Direction (ND). These results are consistent with the data on sheet samples [7].

As materials were cold-deformed (up to 74% reduction-in-thickness) at room temperature, they became stronger because work-hardening was positive. In samples deformed to 45% and 55% reduction-in-thickness, the values of UTS reached 1222 MPa and 1546 MPa, respectively. We did not observe any further strengthening in materials deformed to greater than 74% reduction-in-thickness. This is consistent with our previous observations [7].

TABLE I
RT Tensile Test Results of Samples Deformed to 45%

Test Direction	E 1* (GPa)	E 2* (GPa)	UTS (MPa)	YS (MPa)
LD	184	172	1222	1072
TD	206	194	1273	1123
ND	235	226	1185	949

*E1 and E2 are the Youngs modulus at initial loading and reloading, respectively

In our materials, work-hardening appeared to be anisotropic, leading to different ratios of UTS/YS in different directions. In samples deformed to 45% reduction in thickness, for example, the values of UTS/YS were 13% in both TD and LD (Longitudinal Direction), but the value of UTS/YS was 25% in ND. The anisotropy in mechanical properties was related to texture and planar defects in the materials.

Aging treatment further increased the strength of deformed materials. In some samples of materials subjected to aging heat treatment after they had been deformed to 55% reduction-in-thickness, UTS reached 1748 MPa. This was a 10% increase over the UTS of deformed samples that had not been aged. We noticed that insufficient ventilation during the aging process reduced the achievable strength. The UTS reached only 1667 MPa in samples deformed to 55% and then aged thereafter without sufficient ventilation. In samples that had been deformed by rolling to greater than 65% reduction-in-thickness, the aging process further improved strength by >20% compared to similar samples without aging. After aging, samples that had been deformed to a higher deformation strain showed higher mechanical strength than samples deformed to a lower deformation strain.

At cryogenic temperature (77 K), the stress -strain curves of materials subjected to uniaxial loading showed the same deformation-hardening features that had appeared at room temperature (Fig. 1).

The biaxial stress of the rolling process introduced an anisotropy of elastic properties. Young's modulus showed the highest values in the ND of the plate and the lowest values in the direction parallel to LD or the rolling direction (Table I). We observed this anisotropy in samples tested at room temperature, at 77 K, and at 4K (Table II).

In our tensile tests, which we performed by applying uniaxial stresses to samples, we found that a difference in deformation mode (i.e., rolling alone vs rolling plus tensile testing) introduced a difference in the Young's modulus. Before testing, our samples had been subjected only to a rolling process that exposed materials to reduction in thickness of 45%, 55%, or 65%. This rolling process subjected materials to biaxial stress rather than the uniaxial stress of tensile tests.

As plastic deformation increased by about 0.2%, the modulus in tensile tests appeared to decrease by up to 10% (Table II). During previous rolling deformation from 45% to 55% or from

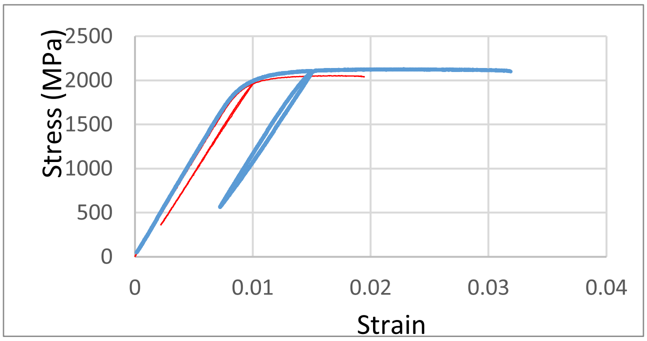

(a)

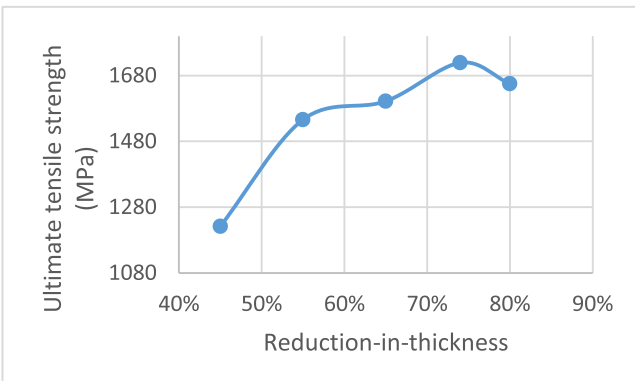

(b)

Fig. 1. (a) Comparison of typical stress strain curves of MP35N sheets deformed to 55% (thin solid line) and 65% (thick solid line). Both samples were aged after deformation. For samples deformed to 65%, the modulus for the initial loading from 0% strain is about 231 GPa and the modulus for the second loading after ~0.5% plastic deformation strain is 217 GPa. For samples deformed to 55%, the modulus for the initial loading from 0% strain is about 220 GPa and the modulus for the second loading after ~0.05% plastic deformation strain is 211 GPa. Both tests were undertaken at 77 K with the tensile axis parallel to the rolling direction (RD). (b) Strength vs deformation strain.

TABLE II
TENSILE TEST RESULTS OF SAMPLES DEFORMED TO 65% AND THEN AGED

Test Orientation	T (K)	Modulus (GPa)
AG-LD	77	224±19
AG-TD	77	263±19
AG-LD	4	236±32
AG-TD	4	264±15

55% to 65% reduction in thickness, however, these same samples had already been subjected to biaxial rather than uniaxial stresses, with the result that the modulus of samples deformed to 65% was higher than that of samples deformed to 55% and 45%.

B. Microstructure

The microstructure of as-rolled samples showed a high density of planar defects (in addition to the dislocations expected in any face-centred-cubic, deformed material). Our analyses indicated that these planar defects were either stacking faults or twins. The distance between these planar defects was about 50 nm, and their length ranged from 100 to 500 nm. We believe that the high density of planar defects played a major role in strengthening the materials at both room and cryogenic temperatures.

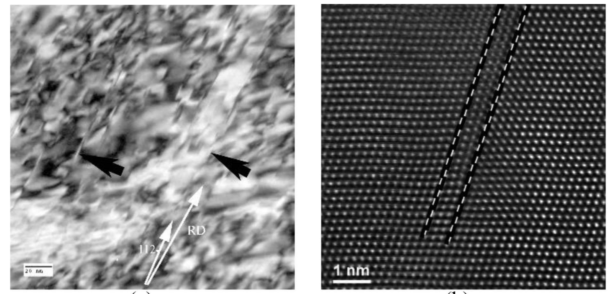

(a) (b)

Fig. 2. Microstructure in samples deformed to 65% and aged at 550 °C for 8 hours. (a). Bright field TEM image. Selected stacking faults are indicated by black arrows. White arrows show that rolling direction (RD) is parallel to <112> orientation. (b). Atomic resolution STEM-HAADF image showing a stacking fault. The zone axis for imaging is in [011]. The bright dots show columns of atoms. Two dashed lines show a stacking fault.

Similarly, the microstructure of samples that had been both rolled and aged showed a high density of stacking faults and/or twins (Fig. 2). In all samples, the density of planar defects increased with deformation strain, but there was no obvious difference between aged samples and those that had been deformed but not aged.

We observed that the formation of planar defects in our samples occurred in more than one habit plane. We measured the angles between habit planes and the rolling direction and found that most of them were about 0 and 60 degrees. Such orientation may play a role in the anisotropy that we observed in mechanical properties.

Previous researchers have observed either element-segregation or precipitate-formation in deformed and aged wire samples. These researchers have suggested that the major element that leads to segregation or precipitation is Mo [41]. To see whether these results, particularly Mo segregation, apply also to sheet samples, we used atomic resolution High-Angle Annular Dark-Field (HAADF) STEM imaging to compare samples that had been deformed to samples that had been both deformed and aged. Our data showed that most of the stacking faults stood alone. The thickness of a single stacking fault was only one to three atomic layers. We found no significant change in image contrast between the atomic columns located within grains and those located on the planar defects themselves [42]. There was no evidence of Mo element segregation or precipitation in our STEM-HAADF data. Because the atomic Z numbers of Ni, Co, and Cr fall in a very narrow range, however, we could not determine from HAADF-STEM images whether segregation of Cr and Co occurred on stacking fault planes.

Magnetic property measurement at temperatures above 77 K of as-rolled samples (some without aging, others with aging) demonstrated that aging introduced ferromagnetic ordering. All of the as-rolled samples had entirely paramagnetic properties. Aged samples, however, had magnetic properties similar to those of a composite with both paramagnetic and ferromagnetic components. The coercivity of the aged samples was only 200 Oe [43]. Assuming that these aged samples were indeed composed of two components, this coercivity value would indicate that the ferromagnetic component had a very small volume fraction, like the volume fraction of the stacking faults. The change from paramagnetic to ferromagnetic ordering may have contributed to age-strengthening. Further work, using atomic resolution EELS mapping, is underway to ascertain whether the strengthening of the aged samples was the result of magnetic ordering or alloying segregation.

IV. Discussion

In both annealed condition and as-deformed condition, we observed neither elemental segregation nor phase separation in our alloy. Consequently. we chose to model the entropy of this alloy as an ideal solution, i.e., one in which the thermodynamic properties are analogous to those found in a mixture of ideal gases. As an ideal solution, this alloy seemed to us to have met an important criterion for the category of High Entropy Alloy (HEA). Its calculated configuration entropy, however, was only 1.25R, which has led some other researchers to instead consider this alloy a Medium Entropy Alloy (MEA) [44]. These researchers have focused on the fact that the activation energy of recrystallization and the activation energy of grain growth are very similar to the activation energy of self-diffusion in MEAs. Researchers, of course, are very interested in both MEAs and HEAs because of their high achievable mechanical strength. Based on our studies of samples deformed to various levels of deformation strain and subsequently heat-treated at different temperatures for different times, the high strength of MP35N has been attributed largely to a high density of planar defects (twins and stacking faults). We have observed that achievable strength in MP35N, particularly at cryogenic temperatures, is considerably higher than in most of the HEAs and MEAs studied so far.

We found that, in other alloys with face-centred cubic structure matrices, strengthening resulted from the introduction of deformation-induced precipitates and dislocations [11], [45], [46], [47], [48], [49], [50]. In MP35N, however, strengthening resulted from the introduction of deformation-induced planar defects rather than precipitates. The distance between these planar defects was only about 50 nm, small enough to restrict the motion of dislocations at low stress levels and thus provide high strength to the alloys.

In our alloy, the sample that was both deformed and aged exhibited an electrical resistivity higher by $0.7 \times 10^{-8}\Omega$m and a magnetic susceptibility higher by 0.005 at 25 K compared to the sample that was only deformed. This suggests that the aging process produces an internal structural change that leads to a greater scattering of transport electrons. Other researchers have attributed this stronger scattering to the segregation of certain alloying elements in wire samples [41], [43]. Some researchers have found segregation of Mo, Al, and Cr in wires of MP159 and MP35N alloys [41], [51], [52]. In our MP35N sheets, however, we observed no evidence of segregation.

At cryogenic temperatures, our MP35N sheets became stronger. Other researchers have attributed cryogenic strengthening in MP35N to grain refinement [53]. In our sheets, however, grain refinement did not appear. We attributed cryogenic strengthening instead to a phenomenon we have observed in other fcc materials–the suppression of dynamic recovery [42].

Plastic deformation appeared to change the Young's modulus of our alloy. Other researchers have found that plastic deformation reduces the modulus in alloys with similar chemistry [18], [51]. In our alloy, however, we observed more complex behaviour. The modulus was higher in samples that had been subjected to large plastic deformation but not to age-hardening. In samples that had previously undergone deformation followed by aging, however, the modulus was reduced when we subjected these same samples to additional plastic deformation. Such behaviour may be related to internal stresses resulting from the formation of more and more planar defects.

Fabrication parameters significantly affected the cryogenic properties of our MP35N alloys. The strengthening effect of aging increased progressively in samples subjected to higher and higher deformation strain. The strengthening effect of aging in samples tested at 77 K, for example, was at its lowest when deformation strain was kept below 45% and reached its maximum when deformation strain rose to 65%.

V. Conclusion

Deformation of Co-Ni-Mo-Cr produced stacking faults and twins, which strengthened the alloy. Increasing the deformation strain to 74% increased the strength of the alloy at both room and cryogenic temperatures. Strength showed anisotropy in deformed samples. In the rolled plate, samples showed highest strength in transverse direction and lowest strength in normal direction. Young's modulus showed similar anisotropy. We attribute this anisotropy to both the texture of the matrix and orientation of the deformation-induced nanoplatelets. Young's modulus was increased by introducing biaxial deformation strain but decreased by introducing uniaxial deformation strain. Aging of deformed samples appeared to make the alloy stronger at both room and cryogenic temperatures. We attribute this age strengthening to internal ordering in the deformation-induced nanoplatelets.

Acknowledgment

The authors thank Mary Tyler for editing and Doan Ngoc Nguyen for discussions and sample preparations.

References

[1] C. M. Chen, A. Bartholf, and E. D. Verink, "Corrosion behavior of MP35N alloy," *J. Electrochem. Soc.*, vol. 123, no. 8, pp. C245–C246, 1976.

[2] A. Gachter, J. Galante, and W. Rostoker, "MP35N - corrosion-resistant, high-strength alloy for orthopedic or surgical implants: Two-year bioassay results," *J. Biomed. Mater. Res.*, vol. 10, no. 5, pp. 829–831, 1976.

[3] J. P. Stroup, A. H. Bauman, and A. Simkovich, "Multiphase MP35N - alloy for deep sour well service," *Mater. Perform.*, vol. 15, no. 6, pp. 43–47, 1976.

[4] F. Escalas et al., "MP35N - corrosion-resistant, high-strength alloy for orthopedic surgical implants - bioassay results," *J. Biomed. Mater. Res.*, vol. 9, no. 3, pp. 303–313, 1975.
[5] P. Altman and D. Hoffmann, "Implantable electrical conductor flexure fatigue issues," in *Proc. 18th Annu. Int. Conf. IEEE Eng.–Med.–AMD-Biol.-Soc.*, 1996, pp. 183–184.
[6] P. A. Altman et al., "Rotary bending fatigue of coils and wires used in cardiac lead design," *J. Biomed. Mater. Res.*, vol. 43, no. 1, pp. 21–37, 1998.
[7] A. Ishmaku and K. Han, "Characterization of cold-rolled and aged MP35N alloys," *Mater. Characterization*, vol. 47, no. 2, pp. 139–148, 2001.
[8] L. Li et al., "Insert coil design of the first 100 T non-destructive magnet," *IEEE Trans. Appl. Supercond.*, vol. 10, no. 1, pp. 518–521, Mar. 2000.
[9] K. Han et al., "Selected Ni alloy considerations for superconducting magnets," *IEEE Trans. Appl. Supercond.*, vol. 23, no. 3, Jun. 2013, Art. no. 7800204.
[10] K. Han, P. Mao, and Y. Xin, "Age-hardening process featuring anomalous aging time," US Patent 10,626,488, 2020.
[11] K. Han et al., "Effects of winding strain and heat treatment on properties of 316 LN and Haynes 242," in *Proc. Amer. Inst. Phys. Conf.*, 2008, pp. 84–91.
[12] I. Haynes, Accessed: Feb. 2, 2019. [Online]. Available: https://www.haynesintl.com/alloys/alloy-portfolio_/High-temperature-Alloys/HAYNES-242-Alloy/principal-features.aspx
[13] R. P. Walsh, K. Han, and V. J. Toplosky, "Fracture toughness measurements and assessment of thin walled conduit alloys in a CICC application," in *Proc. Amer. Inst. Phys. Conf.*, 2008, pp. 68–75.
[14] R. P. Walsh et al., "Effect of an aging heat treatment on the 4 K fracture and fatigue properties of 316 LN and Haynes 242," in *Proc. Amer. Inst. Phys. Conf.*, 2006, pp. 107–114.
[15] M. Raghavan and B. J. Berkowitz, "Tem investigation of phase-transformations in MP35N alloy," *J. Met.*, vol. 31, no. 8, pp. F34–F34, 1979.
[16] M. Raghavan, B. J. Berkowitz, and R. D. Kane, "Transmission electron-microscopic investigation of phase-transformations in MP35N," *Metallurgical Trans. Phys. Metall. Mater. Sci.*, vol. 11, no. 1, pp. 203–207, 1980.
[17] G. Fitzsimons and H. A. Kuhn, "Flow and fracture of a multiphase alloy MP35N for study of workability," *Metallurgical Trans. Phys. Metall. Mater. Sci.*, vol. 15, no. 10, pp. 1837–1847, 1984.
[18] M. Prasad, M. W. Reiterer, and K. S. Kumar, "Microstructure and mechanical behavior of annealed MP35N alloy wire," *Mater. Sci. Eng. Struct. Mater. Properties Microstructure Process.*, vol. 636, pp. 340–351, 2015.
[19] R. Cosimati and D. Mari, "Effects of precipitation hardedning in Co-Ni-Cr alloy on dissipative motion of dislocations by amplitude-dependent internal friction measurements," *Arch. Metall. Mater.*, vol. 60, no. 4, pp. 3077–3081, 2015.
[20] R. Cosimati and D. Mari, "Secondary hardening in Co-Ni-Cr super-alloy investigated by mechanical spectroscopy," *Mater. Sci. Eng. Struct. Mater. Properties Microstructure Process.*, vol. 662, pp. 426–431, 2016.
[21] R. P. Singh and R. D. Doherty, "Strengthening in multiphase (MP35N) alloy .1. AMBIENT-temperature deformation and recrystallization," *Metallurgical Trans. Phys. Metall. Mater. Sci.*, vol. 23, no. 1, pp. 307–319, 1992.
[22] R. P. Singh and R. D. Doherty, "Strengthening in MULTIPHASE (MP35N) alloy: Part II. Elevated temperature tensile and creep deformation," *Metallurgical Trans. Phys. Metall. Mater. Sci.*, vol. 23, no. 1, pp. 321–334, 1992.
[23] A. C. Hood, "MP35N - a multiphase alloy for high-strength fasteners," *Metal Prog.*, vol. 93, no. 5, pp. 81–84, 1968.
[24] C. N. Younkin, "Multiphase MP35N Alloy for medical implants," *J. Biomed. Mater. Res.*, vol. 8, no. 3, pp. 219–226, 1974.
[25] M. Fitzka et al., "Ultrasonic fatigue testing of thin MP35N alloy wire," in *Proc. 21st Eur. Conf. Fracture*, 2016. pp. 1039–1046.
[26] C. J. Gardner et al., "Controlled metallic nanopillars for low impedance biomedical electrode," *Acta Biomaterialia*, vol. 10, no. 5, pp. 2296–2303, 2014.
[27] H. Ghiasi and S. Asgari, "Aging behavior and microstructure evolution of a cold-drawn Ni-Co superalloy," *Scientia Iranica*, vol. 22, no. 1, pp. 281–285, 2015.
[28] S. Q. Lu et al., "Hardening mechanism of MP159 alloy induced by aging," *Trans. Nonferrous Met. Soc. China*, vol. 12, no. 2, pp. 256–259, 2002.
[29] K. Han, J. R. Sims, C. A. Swanson, and H. J. Schneider-Muntau, "Reinforcement materials for high field magnets," *IEEE Trans. Appl. Supercond.*, vol. 14, no. 2, pp. 1141–1144, Jun. 2004.
[30] A. Ishmaku and K. Han, "Deformation induced nanostructure and texture in MP35N alloys," *J. Mater. Sci.*, vol. 39, no. 16/17, pp. 5417–5420, 2004.
[31] S. Asgari et al., "Strain hardening regimes and microstructural evolution during large strain compression of low stacking fault energy FCC alloys that form deformation twins," *Metallurgical Mater. Trans. Phys. Metall. Mater. Sci.*, vol. 28, no. 9, pp. 1781–1795, 1997.
[32] K. Han, V. Toplosky, N. Min, J. Lu, Y. Xin, and R. Walsh, "High modulus reinforcement alloys," *IEEE Trans. Appl. Supercond.*, vol. 28, no. 3, Apr. 2018, Art. no. 0602405.
[33] P. Mao, Y. Xin, and K. Han, "Anomalous aging behavior of a Ni–Mo–Cr–Re alloy," *Mater. Sci. Eng., A*, vol. 556, pp. 734–740, 2012.
[34] P. R. Okamoto and G. Thomas, "Short range order in Ni-Mo alloys - structural considerations," *Mater. Res. Bull.*, vol. 6, no. 1 pp. 45–49, 1971.
[35] B. Fultz et al., "Cryogenic mechanical-properties of Superalloy MP35N," *Cryogenics*, vol. 24, no. 12, pp. 687–690, 1984.
[36] K. Han, "Property of ultrafine grained engineering materials related to high magnetic fields," *Ultrafine Grained Mater. IV*, pp. 473–480, 2006.
[37] K. Han et al., "Mechanical properties of MP35N as a reinforcement material for pulsed magnets," *IEEE Trans. Appl. Supercond.*, vol. 12, no. 1, pp. 1244–1247, Mar. 2002.
[38] V. J. Toplosky and K. Han, "Mechanical properties of Cold-rolled and aged MP35N alloys for cryogenic magnet applications," *Adv. Cryogenic Eng.*, vol. 58, pp. 125–132, 2012.
[39] Y. Xin et al., "Facility implementation and comparative performance evaluation of probe-corrected TEM/STEM with Schottky and cold field emission illumination," *Microsc. Microanal.*, vol. 19, no. 2, pp. 487–495, 2013.
[40] Y. Xin et al., "Aberration-corrected S/TEM at Florida State University," *Microsc. Today*, vol. 22, no. 3, pp. 42–49, 2014.
[41] S. Antonov et al., "The effect of solute segregation to deformation twin boundaries on the electrical resistivity of a single-phase superalloy," *Scripta Materialia*, vol. 186, pp. 208–212, 2020.
[42] K. Han et al., "High strength and high electrical conductivity bulk Cu," *Philos. Mag.*, vol. 84, no. 34, pp. 3705–3716, 2004.
[43] J. Lu et al., "Low temperature physical properties of Co-35Ni-20Cr-10Mo alloy MP35N," *Cryogenics*, vol. 86, pp. 106–111, 2017.
[44] M. Rezayat and F. Najib, "Grain refinement of CoNiCrMo non-equiatomic medium entropy alloy," *Met. Mater. Int.*, vol. 29, no. 1, pp. 235–246, 2023.
[45] R. Niu et al., "Deformation induced precipitation in CuCrZr composites," *Mater. Sci. Eng., A*, vol. 875, 2023, Art. no. 145092.
[46] R. Niu, V. Toplosky, and K. Han, "Cryogenic temperature properties and secondary phase characterization of CuCrZr composites," *IEEE Trans. Appl. Supercond.*, vol. 32, no. 6, Sep. 2022, Art. no. 4300405.
[47] S. Downey II, P. Kalu, and K. Han, "The effect of heat treatment on the microstructure stability of modified 316LN stainless steel," *Mater. Sci. Eng., A*, vol. 480, no. 1/2, pp. 96–100, 2008.
[48] S. Downey et al., "A study of submicron grain boundary precipitates in ultralow carbon 316 LN steels," *Metallurgical Transaction A*, vol. 41, no. 4, pp. 881–887, 2010.
[49] S. T. Downey et al., "Grain boundary plane distributions in modified 316LN steel exposed at elevated and cryogenic temperatures," *J. Mater. Sci.*, vol. 42, no. 23, pp. 9543–9547, 2007.
[50] R. P. Walsh et al., "The low temperature mechanical properties of a Nitronic 40 forging," in *Proc. IOP Conf. Ser.: Mater. Sci. Eng.*, 2020.
[51] Q. K. Zhang et al., "Severe elastic modulus shift of deformed CoNiCrMo alloy under relative low-temperature exposure," *Phys. Rev. B*, vol. 107, no. 2, pp. L020102-1–L020102-5, 2023.
[52] D. Sorensen et al., "Investigation of secondary hardening in Co-35Ni-20Cr-10Mo alloy using analytical scanning transmission electron microscopy," *Acta Materialia*, vol. 63, pp. 63–72, 2014.
[53] W. W. Zhang et al., "Microstructure evolution and strengthening mechanisms of MP159 superalloy during room temperature rolling and cryorolling," *J. Alloys Compounds*, vol. 908, 2022, Art. no. 164667.